

Towards understanding cloud response in atmospheric GCMs: the use of tendency diagnostics

T. OGURA¹, S. EMORI^{1,2}, M.J. WEBB⁴, Y. TSUSHIMA², T. YOKOHATA¹, A. ABE-OUCHI^{2,3}, AND M. KIMOTO³

1. National Institute for Environmental Studies, 16-2 Onogawa, Tsukuba, Ibaraki, 305-8506, Japan.

2. Frontier Research Center for Global Change, Japan Agency for Marine-Earth Science and Technology, 3173-25 Showamachi, Kanazawa-ku, Yokohama, Kanagawa 236-0001, Japan.

3. Center for Climate System Research, The University of Tokyo, 5-1-5 Kashiwanoha, Kashiwa, Chiba 277-8568, Japan.

4. Hadley Centre for Climate Prediction and Research, Met Office, FitzRoy Road, Exeter, EX1 3PB, UK.

Submitted to J.M.S.J.

Abstract

In climate change projections, inter-model differences in cloud feedback have been identified as the largest source of uncertainty. The source terms of the cloud condensate tendency equation (CCTD) are expected to be useful diagnostics to better understand the different cloud responses to a CO₂ increase in GCMs. To demonstrate the idea, analysis of the CCTD response to CO₂ doubling is presented using two versions of MIROC3.2 with different climate sensitivities of 6.2°C ('HS' version) and 4.1°C ('LS' version). The model's response to CO₂ doubling is characterized with a marked difference in the cloud feedback between the two versions, which is consistent with the cloud response in the southern middle latitudes: cloud decreases in the HS version and increases in the LS version. Analysis of the source terms reveals that the difference in cloud response is attributable to the ice sedimentation process. The results also suggest the importance of the vertical cloud ice profile which controls the ice sedimentation response to a CO₂ increase, indicating the potential for providing constraints on the aspect of cloud feedback.

1. Introduction

Cloud feedback is still a major source of uncertainty in estimating climate sensitivity ' ΔT_{2x} ', which is defined here as the equilibrium response of surface air temperature to atmospheric CO₂ doubling (Cess et al. 1990, Ringer et al. 2006, Soden and Held 2006). The response of low level clouds, including marine boundary layer clouds in the subtropics, is shown to be a key factor which causes inter-model variance in cloud feedback (Webb et al. 2006, Wyant et al. 2006, Bony and Dufresne 2005). In addition, the importance of the mixed phase cloud response in middle-high latitudes was noted by Tsushima et al. (2006), which is consistent with the previous studies indicating the model dependency of mixed phase cloud feedback (Li and Le Treut 1992, Senior and Mitchell 1993). However, mechanisms responsible for these inter-model spreads in the cloud response are yet to be clarified.

Source terms of the cloud condensate tendency equation in GCMs are expected to be useful diagnostics to tackle this problem. Their advantage is that the cloud condensate response to an increase in CO₂ can be directly related to the physical processes which enhance or retard the response. A model inter-comparison of these diagnostics may help to identify key processes leading to the difference in the cloud responses between GCMs.

In order to illustrate this idea, we compare two versions of an AGCM developed jointly by the Center for Climate System Research (CCSR), National Institute for Environmental Studies (NIES), and Frontier Research Center for Global Change

(FRCGC). One version gives a climate sensitivity of 6.2°C , which is called the Higher Sensitivity version ('HS' hereafter), and the other version yields 4.1°C , which is called the Lower Sensitivity version ('LS' hereafter). The difference between the two versions lies in the treatment of cloud microphysics. Making use of the tendency diagnostics, the present study attempts to describe how the sensitivity difference arises between the HS and LS versions.

The model and experimental design are described in section 2. In section 3, results from the doubled CO_2 experiments are presented. Finally, the implications of the obtained results are summarised and discussed in section 4.

2. Model and experimental design

a. Model

The model used in the present study is the CCSR/NIES/FRCGC AGCM5.7 (K-1 model developers, 2004), which is the atmospheric component of the MIROC3.2 'medres' version used in IPCC's fourth assessment report (AR4). The model resolution is T42 with 20 vertical sigma layers. The non-convective cloud distribution is calculated using a parameterization based on Le Treut and Li (1991), in which the cloud condensate content is calculated by solving a mass budget equation. Processes considered in the mass budget are condensation, precipitation, ice cloud sedimentation and evaporation of both cloud water and rain droplets. Condensation is treated by a statistical method assuming a uniform or 'top-hat' probability distribution of the total water content on a

sub-grid scale. Condensed cloud water is then partitioned into the liquid phase and solid phase according to the local air temperature so that different precipitation rates can be applied to each cloud phase. Liquid precipitation is parameterized based on the method by Berry (1967) as follows:

$$P = -\frac{\partial l_L}{\partial t} = \frac{\alpha \rho l_L^2}{\beta + \gamma \frac{N_c}{\rho l_L}} + C_c F_p l_L, \quad (1)$$

where P is the precipitation rate, l_L is the cloud liquid water content, ρ is the air density, N_c is the cloud droplet number concentration, and F_p is the precipitation flux from the layer above. α , β , γ and C_c are constants. The second term allows for the collection of cloud droplets by precipitation, following Senior and Mitchell (1993). Ice precipitation is represented following Sundqvist (1978):

$$P = C_t \left[1 - \exp \left\{ - \left(\frac{l}{l_c C} \right)^2 \right\} \right] l_F + C_c F_p l_F \quad (2)$$

, where l is the cloud condensate content, l_c is the critical cloud condensate content for rapid snow formation, C is the cloud amount, l_F is the cloud ice content, and C_t is a constant. Sedimentation of ice cloud particles is based on the empirical formula of Heymsfield (1977) as follows:

$$P = \left\{ \frac{V_0 (\rho l_F)^\delta}{\Delta z} \right\} l_F \quad (3)$$

, where Δz is the thickness of the model layer and V_0 and δ are constants. Non-convective clouds in the MIROC are also affected by grid scale advection, mixing due to cumulus convection, and dry convective adjustment.

The cumulus parameterization used in this study is based on Arakawa and Schubert (1974) with several simplifications described by Numaguti et al. (1997). The cloud condensate and cloud amount of convective clouds are derived from the cloud base mass flux calculated in the convection scheme, although the condensate content is generally smaller than that of non-convective clouds by one order of magnitude. Anvil clouds are treated as non-convective clouds in the MIROC.

b. HS and LS versions

The two model versions, HS and LS, are different in three respects (Table 1). Firstly, the temperature range at which the mixed phase cloud exists is different. The mass ratio of liquid cloud water to cloud condensate is specified by an empirical function of the local air temperature as shown in Figure 1. In the HS version, the mixed phase cloud exists between -25°C and -5°C (dashed line), while in the LS version, it exists between -15°C and 0°C (solid line). These two functions are within the range of uncertainty as suggested by field and satellite observations (Mitchell et al. 1989, Gregory and Morris 1996, Del Genio et al. 1996, Doutriaux-Boucher and Quaas 2004).

Secondly, the treatment of fallen cloud ice is different. The ice sedimentation, represented by equation (3), causes cloud ice to fall from the upper layers to lower layers at each time step. In the HS version, the fallen cloud ice is diagnosed as liquid clouds suspended in the air between the temperature range of -25°C and -5°C , while in the LS version, all the melted cloud particles are classified as rain which falls to the ground in one time step. In addition, falling cloud ice remains in the solid phase until it

reaches the melting point (0°C) in the LS version, which allows cloud ice to exist in the warmer region in the LS version than the HS version.

Thirdly, the specified parameter values related to the precipitation efficiency are different. Since the ice sedimentation process is more effective in the LS than the HS version, precipitation is made more efficient in the HS than the LS version to balance the radiation budget at the top of the atmosphere in both versions. The parameters α in equation (1) and V_0 in equation (3) are thus specified as follows: $(\alpha, V_0) = (0.04, 0.5)$ in the HS version and $(\alpha, V_0) = (0.01, 0.25)$ in the LS version.

The two versions' ability to reproduce the present day climatology is comparable, including the cloud radiative forcing evaluated with the ERBE observation (Figure 2). Both versions exhibit substantial errors, especially in the tropics and southern middle latitudes which are too reflective in terms of shortwave. The errors in the tropics are due to the stratocumulus regime which is simulated too often (Williams and Tselioudis 2007). When comparing the cloud ice distribution between the HS and LS versions, there is a marked difference between the two, as shown in Figure 3. We can see that cloud ice exists in lower latitudes/altitudes in the LS than in the HS version, which can be explained by the difference in the mixed phase cloud temperature range and in the treatment of fallen cloud ice. This difference in cloud ice distribution is related to the cloud condensate response to the CO_2 increase, which will be described in Section 3.

c. Design of sensitivity experiments

Both versions of the AGCM are coupled to a 50 m depth slab ocean model and a thermodynamic sea ice model. The coupled GCM is then forced by the oceanic heat flux (Q-flux), calculating the SST and sea ice thickness for 50 years with (a) the external conditions of year 1850 ('control experiment' hereafter) and with (b) doubled CO₂ concentration ('2 × CO₂ experiment' hereafter). The last 10 years of each integration are considered in a quasi-equilibrium state and are used to make a climatology. The equilibrium response to CO₂ doubling is assessed based on this climatology, which gives the ΔT_{2x} values of 6.2°C for the HS version and 4.1°C for the LS version.

We should note here that the climate sensitivity of 4.1°C (LS version) is higher than most other climate models in IPCC's AR4. The higher sensitivity of LS is mainly attributed to the more positive cloud feedback, which is related to the larger reduction in low level cloud and shortwave cloud radiative forcing (Webb et al. 2006). The response of the marine boundary layer cloud is shown to be a major factor contributing to the inter-model variance, as noted in the Introduction.

d. Additional experiments (MS1 and MS2 versions)

In order to identify factors contributing to the difference in climate sensitivity between the HS and LS versions, the control and 2 × CO₂ experiments (including the calibration run to obtain Q-flux) are repeated with two additional settings, MS1 and MS2 (Table 1).

The only difference between the HS, MS1, MS2, and LS versions lies in the cloud microphysical assumptions described in subsection 2b. Hence, we can attribute the difference in ΔT_{2x} between the four versions to (i) the temperature range for mixed phase clouds, (ii) the melted cloud ice treatment, and (iii) parameter adjustment, the contributions of which are 1.2°C, 1.1°C, and -0.2°C, respectively (Table 1). To explain the difference between the HS and LS versions, therefore, we may focus on the impact of (i) and (ii) by referring to the results of the HS, MS2, and LS versions. The HS version is taken to be equivalent to MS1 because the cloud response, as well as climate sensitivity, of the MS1 version is similar to that of the HS version.

3. Results

The response of MIROC3.2 to CO₂ doubling is characterized by the large difference in cloud feedback between the HS, MS2, and LS versions. Figure 4(a) illustrates the shortwave cloud feedback in the DJF season, evaluated by the response of cloud radiative forcing normalized by climate sensitivity (Boer and Yu 2003, Webb et al. 2006). Large positive feedback can be seen in the HS version in the southern middle latitudes, while the corresponding feedbacks in the MS2 and LS versions are smaller or negative, which is consistent with the difference in climate sensitivity. A similar difference in cloud feedback can be seen in the northern middle latitudes during the JJA season as well, although its magnitude is smaller than that in the southern hemisphere. We should note that the cloud feedback shown here may be affected by changes in factors other than clouds, such as sea ice ('cloud masking effect', Soden et al. 2004). However, the sea ice distribution is restricted to high latitudes during DJF, and the difference in cloud feedback can be seen outside the range of the sea ice extent, indicating the importance of cloud response.

The response of cloud condensate to CO₂ doubling is also different between the three versions, as illustrated in Figures 4(b–d). Overall, cloud condensate decreases (increases) in low (high) latitudes, which is a feature common to the three versions. However, the cloud condensate decrease in the HS version is large and extends to high latitudes as far as 65°S, while the decrease in the MS2 and LS versions is relatively small and is restricted to lower latitudes up to 50°S. This difference in cloud response is consistent with the shortwave cloud feedback which is positive in the HS version and is more negative in the MS2 and LS versions. Analyzing the source and sink terms of the cloud condensate tendency equation may be useful to understand the difference in cloud responses between the three versions.

The cloud condensate tendency equation of MIROC3.2 is written conceptually as follows:

$$\frac{\partial Q_c}{\partial t} = [\text{a. Condensation, evaporation, precipitation}] + [\text{b. Ice sedimentation}] + [\text{c. Advection}] + [\text{d. Cumulus mixing}] + [\text{e. Dry convective adjustment}] \quad (2)$$

, where Q_c is the non-convective cloud condensate in [kg/kg]. Convective cloud condensate is omitted for simplicity because it is much less than the non-convective component as noted in section 2. Terms on the RHS are evaluated by taking cloud increments at various stages of calculating the model physics. The cloud condensate tendency, $\frac{\partial Q_c}{\partial t}$, is equal to zero in an equilibrium state. It becomes positive, however, when Q_c increases in response to CO₂ doubling, which is due to some source terms on the RHS becoming larger (or sink terms becoming smaller) compared to the equilibrium state. The terms making a positive contribution to the Q_c tendency are thus regarded as ‘driving’ the cloud response. In this way, we may be able to identify key processes which lead to the difference in cloud responses between the HS, MS2, and LS versions. The terms on the RHS of equation (2) are hereafter referred to as the cloud condensate tendency diagnostics (CCTD).

To demonstrate the idea, we first focus on the shaded region in Figure 4 (50°S – 64°S , $\sigma = 0.96$ – 0.78), where the inter-model variance in the cloud response is pronounced. The equilibrium response of both the cloud condensate and the CCTD averaged over this shaded region is displayed in Figure 5. The remarkable feature is that all the cloud condensate responses—decrease in the HS version and increase in both the MS2 and LS versions—are driven by the same term: CCTD(b), the ice sedimentation term. It is suggested that ice sedimentation is the key process which drives the cloud response in the LS and MS2 versions but drives it in the opposite direction in the HS version. It is also interesting to note that CCTD(a) tends to counter-act the ice sedimentation term CCTD(b), retarding the cloud condensate responses. This balancing effect can be explained by the evaporation and vertical eddy diffusion included in CCTD(a), both of which tend to dampen the cloud variation.

The comparison of the CCTD is extended to the transient state as well because the difference in cloud responses between the three versions is more relevant to the processes driving the transient response rather than those maintaining the equilibrium states. The temporal correlation is calculated between the responses of the cloud condensate and the CCTDs at each grid point, using the time series from the first 20 years after the instantaneous CO_2 doubling, sampled every DJF season. A CCTD with positive correlation is interpreted as driving the cloud response, while one with negative correlation retards it. The zonal mean distribution of the correlation is shown in Figure 6(a–c) for CCTD(b), the ice sedimentation term. Note that the negative correlation is eliminated by assigning zero values in the figures because we are concerned with the processes driving the cloud response. Furthermore, the sign of the coefficients are

switched to negative when the cloud responses are negative so that we can distinguish between the region in which the cloud condensate decreases and that in which the cloud condensate increases.

Figures 6(a–c) illustrate the two layered pattern of the ice sedimentation influence on the cloud condensate; the increase is driven above and the decrease is driven below. The difference between the three versions can be seen in the latitudinal extent of the pattern. The negative values in the HS version extends to the high latitudes as far as 65°S while they are restricted to lower latitudes as far as 50°S in the MS2 and LS versions, leading to the opposite roles of the ice sedimentation process in the shaded region, which is consistent with the equilibrium response (Figure 5).

The different spatial patterns of the ice sedimentation influence as shown in Figure 6 could be related to the difference in the control cloud ice distribution (Figure 3). This idea is described in more detail using a conceptual model in Figure 7. The conceptual model consists of grid boxes in three consecutive vertical layers, $k - 1$, k , and $k + 1$, with each box containing cloud ice content Q_{ice}^k (at level k), which controls the sedimentation flux to below, as $F_{ice}^k = C \cdot Q_{ice}^k$. For simplicity, C is assumed constant. In response to CO₂ doubling, cloud ice content decreases by $\Delta Q_{ice}^k (< 0)$ due to melting, which leads to a reduction in the downward ice flux at each level. The response of the ice flux convergence at level k equals $\Delta(F_{ice}^{k+1} - F_{ice}^k) = C \cdot (\Delta Q_{ice}^{k+1} - \Delta Q_{ice}^k)$. If the vertical gradient of the cloud ice reduction is positive ($\frac{\Delta Q_{ice}^{k+1} - \Delta Q_{ice}^k}{\Delta z} > 0$), the flux convergence at level k will increase ($\Delta(F_{ice}^{k+1} - F_{ice}^k) > 0$). Hence, the response of the ice

flux convergence (i.e. response of the ice sedimentation term, $\Delta \text{CCTD}(b)$) is controlled by the vertical gradient of cloud ice reduction.

The results of MIROC3.2 appear to be consistent with this simple argument, as illustrated in Figure 8. The thick curves in Figure 8 show the vertical profiles of the cloud ice response averaged over the latitude band 50°S – 64°S in DJF. If we focus on the shaded region where the inter-model variance in the cloud response is large (as noted in Figure 4), we notice that the vertical gradient of the cloud ice reduction is negative for the HS version (solid), positive for the LS version (dotted), and rather neutral for the MS2 version (dashed). Hence, the different responses of the ice sedimentation between the three versions as seen in Figures 5 and 6 are consistent with the vertical profiles of the cloud ice response. We note here that the increase in ice flux convergence in the LS version leads to an increase in liquid clouds because the thermodynamic phase of the increased cloud condensate is determined by the temperature dependent function (Figure 1).

It is also shown in Figure 8 that the vertical profiles of the cloud ice response (thick curves) closely follow those of the control cloud ice distribution (thin curves) in the lower troposphere. If the maximum of the control cloud ice is located near the surface as in the LS version (dotted curve), the maximum of the ice reduction will also be located near the surface because more ice is susceptible to melting near the surface, which makes the vertical gradient of the cloud ice reduction positive except very near the surface. If the maximum of the control cloud ice is located well above the surface as in

the HS version (solid curve), the vertical gradient of the ice reduction will be negative near the surface because all the ice melts away.

Therefore, it is suggested that the vertical profile of the control cloud ice content is one of the key elements to understand the different responses in ice sedimentation and cloud condensate between the HS, MS2, and LS versions. As noted in section 2, the difference in the control cloud ice distribution is attributed to the model settings related to the non-convective cloud parameterization. The cloud ice increase in the MS2 version relative to the HS version (thin curves in Figure 8) is related to the treatment of fallen cloud ice which permits the ice to remain in the solid phase until it reaches 0°C. Further increase in cloud ice in the LS version relative to the MS2 version is due to the temperature range for the mixed phase cloud in which more condensate is diagnosed as ice cloud.

The obtained results also imply that evaluating the vertical cloud ice profile through observation can potentially constrain the simulated cloud phase feedback, at least in the present versions of MIROC3.2. The observed profile of cloud ice content is becoming available from the spaceborne radar/lidar instruments in the CloudSat and CALIPSO missions (Stephens et al. 2002, Mace et al. 2007). The model clouds may also be evaluated using the ground-based measurements as conducted in the Cloudnet project (Illingworth et al. 2007) and the Atmospheric Radiation Measurement (ARM) programme (e.g. Xie et al. 2005). Together with the CloudSat and CALIPSO simulator to support the comparison of satellite data with the model output (Bodas-Salcedo 2007), these observations are expected to result in better understanding and evaluation of cloud feedback.

4. Summary and discussion

The source terms of the cloud condensate tendency equation (CCTD) are expected to be useful diagnostics to better understand the cloud response to a CO₂ increase in GCMs. To demonstrate this idea, analysis of the CCTD response to CO₂ doubling is presented using three versions of MIROC3.2 with different climate sensitivities—6.2°C (HS version), 5.3°C (MS2 version), and 4.1°C (LS version). The model's response to CO₂ doubling is characterized with a large difference in the cloud feedback between the three versions, which is consistent with the difference in cloud response in the southern middle latitudes. The present CCTD analysis revealed that the difference in cloud response results from the ice sedimentation process which drives a cloud decrease in the HS version while it drives a cloud increase in the MS2 and LS versions. The dissimilar roles of the ice sedimentation reflect the difference in vertical cloud ice profiles which control the vertical ice flux responding to an increase in CO₂.

The results of the present study illustrate the advantage of obtaining the CCTD from GCMs. The process driving the cloud response is identified for different versions of MIROC3.2, which helps to understand the differences in cloud response and in cloud feedback. Although the present study deals with an example in the southern middle latitudes, this method is applicable to other regions as well, where processes other than ice sedimentation are dominant. In particular, a model inter-comparison of low level clouds in low latitudes is needed to understand the source of uncertainty in cloud feedback of IPCC's AR4 models.

One remaining problem is that the definition of the CCTD is dependent on the structure of cloud parameterization. Hence, a comparison between GCMs with different cloud parameterization may not be as straightforward as in this study. However, the preliminary results of the CCTD inter-comparison between MIROC3.2 and the Hadley Centre GCM (HadGEM1) appear to be promising, giving some insight into the

difference in the mixed phase cloud feedback, which are to be presented in a separate paper.

Another problem is that only limited information is available on the factors controlling the condensation, evaporation, and precipitation term, CCTD(a). Since this term plays a dominant role in low latitudes, it is desirable that the definition of CCTD(a) is updated so that its variation can be explained by the contribution from various factors such as radiation and boundary layer mixing.

Despite the difficulty and limitations as noted above, we still argue that the tendency diagnostics have the potential to complement other feedback analysis techniques (e.g. Taylor et al. 2007, Yokohata et al. 2005, Boer and Yu 2003) and help to understand the source of uncertainty in cloud feedback. It is hoped that the model inter-comparison will be extended to a wider range of GCMs. A collaboration with other modelling groups in the framework of the Cloud Feedback Model Intercomparison Project (CFMIP) is being prepared and will be the theme of the future study.

In the present study, it is also suggested that the cloud response to a CO₂ increase is sensitive to the vertical profile of the control cloud ice content. This result is consistent with Li and Le Treut (1992) and Senior and Mitchell (1993), who demonstrated the dependence of the cloud response on the cloud phase diagnosis and ice fall velocity. Improvement in cloud ice simulation is therefore crucial to increase our confidence in the projection of future climate change. The evaluation of model cloud ice with observed vertical profiles, which are available from satellite and ground-based lidar/radar measurements, is expected to have a large impact on constraining the cloud feedback.

Acknowledgements

The authors would like to thank Catherine Senior and William Ingram for their helpful comments. Thanks are due also to an anonymous reviewer whose suggestions led to improvements in the manuscript. This work was funded by Research Revolution 2002

(RR2002) from the Ministry of Education, Culture, Sports, Science and Technology of Japan. It was also supported by the visiting scientist program at the UK Meteorological Office. The Earth Simulator and an NEC SX-6 at NIES were employed to perform the AGCM runs.

Reference

- Arakawa, A. and W.H. Schubert, 1974: Interactions of cumulus cloud ensemble with the large-scale environment. Part I. *J. Atmos. Sci.* 31, 671-701.
- Berry, E.X., 1967: Cloud droplet growth by collection. *J. Atmos. Sci.* 24, 688-701.
- Bodas-Salcedo, A., 2007: Delivery of CloudSat/CALIPSO simulator enabling space-based radar and lidar measurements to be simulated in climate models. Defra Milestone 06/07 07.02.06, Hadley Centre, Clouds, water vapour and radiation 23/03/07.
- Boer, G. J. and B. Yu, 2003: Climate sensitivity and response. *Clim. Dyn.*, 20, 415-429.
- Bony, S. and J. -L. Dufresne, 2005: Marine boundary layer clouds at the heart of tropical cloud feedback uncertainties in climate models. *Geophys. Res. Lett.*, 32, L20806, doi:10.1029/2005GL023851.
- Cess, R.D., G.L. Potter, J.P. Blanchet, G.J. Boer, A.D. Del Genio, M. Deque, V. Dymnikov, V. Galin, W.L. Gates, S.J. Ghan, J.T. Kiehl, A.A. Lacis, H. Le Treut, Z.X. Li, X.Z. Liang, B.J. McAvaney, V.P. Meleshko, J.F.B. Mitchell, J-J. Morcrette, D.A. Randall, L. Rikus, E. Roeckner, J.F. Royer, U. Schlese, D.A. Sheinin, A. Slingo, A.P. Sokolov, K.E. Taylor, W.M. Washington, R.T. Wetherald, I. Yagai, M.H. Zhang, 1990: Intercomparison and interpretation of climate feedback processes in 19 atmospheric general circulation models. *J. Geophys. Res.* 95, 16601-16615.
- Del Genio, A.D., M.S. Yao, W. Kovari, K.K.W. Lo, 1996: A prognostic cloud water parameterization for global climate models. *J. Clim.* 9, 270-304.
- Doutriaux-Boucher, M. and J. Quaas, 2004: Evaluation of cloud thermodynamic phase parameterizations in the LMDZ GCM by using POLDER satellite data. *Geophys. Res. Lett.* 31, L06126, doi:10.1029/2003GL019095.
- Gregory, D. and D. Morris, 1996: The sensitivity of climate simulations to the specification of mixed phase clouds. *Clim. Dyn.* 12, 641-651.

- Heymsfield, A.J., 1977: Precipitation development in stratiform ice clouds. *J. Atmos. Sci.* 34, 367-381.
- Illingworth, A.J., R.J.Hogan, E.J.O'Connor, D.Bouniol, M.E.Brooks, J.Delanoë, D.P.Donovan, J.D.Eastment, N.Gaussiat, J.W.F.Goddard, M.Haeffelin, H.Klein Baltink, O.A.Krasnov, J.Pelon, J.-M.Piriou, A.Protat, H.W.J.Russchenberg, A.Seifert, A.M.Tompkins, G.-J. van Zadelhoff, F.Vinit, U.Willén, D.R.Wilson, C.L.Wrench, 2007: Cloudnet: Continuous evaluation of cloud profiles in seven operational models using ground-based observations. *Bull. Amer. Meteor. Soc.* 88(6), 883-898.
- K-1 model developers, 2004: K-1 coupled model (MIROC) description. K-1 technical report 1, H. Hasumi and S. Emori (Eds.), Center for Climate System Research, the University of Tokyo, 34pp.
- Le Treut, H. and Z.X. Li, 1991: Sensitivity of an atmospheric general circulation model to prescribed SST changes: feedback effects associated with the simulation of cloud optical properties. *Clim. Dyn.* 5, 175-187.
- Li, Z.X. and H. Le Treut, 1992: Cloud-radiation feedbacks in a general circulation model and their dependence on cloud modelling assumptions. *Clim. Dyn.* 7, 133-139.
- Mace, G.G., R.Marchand, Q.Q.Zhang, G.Stephens, 2007: Global hydrometeor occurrence as observed by CloudSat: Initial observations from summer 2006. *Geophys.Res.Lett.* 34, L09808, doi:10.1029/2006GL029017.
- Mitchell, J.F.B., C.A. Senior, W.J. Ingram, 1989: CO₂ and climate: A missing Feedback? *Nature* 341, 132-134.
- Numaguti, A., M. Takahashi, T. Nakajima and A. Sumi, 1997: Description of CCSR/NIES atmospheric general circulation model. CGER's Supercomputer monograph report, Center for Global Environmental Research, National Institute for Environmental Studies, 3, 1-48.
- Ringer, M. A., B. J. McAvaney, N. Andronova, L. E. Buja, M. Esch, W. J. Ingram, B. Li, J. Quaas, E. Roeckner, C. A. Senior, B. J. Soden, E. M. Volodin, M. J. Webb, K. D. Williams, 2006: Global mean cloud feedbacks in idealized climate change experiments. *Geophys. Res. Lett.* 33, L07718, doi:10.1029/2005GL025370.
- Senior, C.A. and J.F.B. Mitchell, 1993: CO₂ and climate: The impact of cloud parameterization. *J. Clim.* 6, 393-418.

- Soden, B. J., A. J. Broccoli, R. S. Hemler, 2004: On the use of cloud forcing to estimate cloud feedback. *J. Clim.* 19, 3661-3665.
- Soden, B. J. and I. M. Held, 2006: An assessment of climate feedbacks in coupled ocean-atmosphere models. *J. Clim.* 19, 3354-3360.
- Stephens, G.L., D.G.Vane, R.J.Boain, G.G.Mace, K.Sassen, Z.Wang, A.J.Illingworth, E.J.O'Connor, W.B.Rossow, S.L.Durden, S.D.Miller, R.T.Austin, A.Benedetti, C.Mitrescu, the CloudSat Science Team, 2002: The CloudSat mission and the A-Train: A new dimension of space-based observations of clouds and precipitation. *Bull. Amer. Meteor. Soc.* 83(12), 1771-1790.
- Sundqvist, H., 1978: A parameterization scheme for non-convective condensation including prediction of cloud water content. *Q. J. R. Meteorol. Soc.* 104, 677-690.
- Taylor, K. E., M. Crucifix, P. Braconnot, C. D. Hewitt, C. Doutriaux, A. J. Broccoli, J. F. B. Mitchell, M. J. Webb, 2007: Estimating shortwave radiative forcing and response in climate models. *J. Clim.* 20, 2530-2543.
- Tsushima, Y., S. Emori, T. Ogura, M. Kimoto, M. J. Webb, K. D. Williams, M. A. Ringer, B. J. Soden, B. Li, N. Andronova, 2006: Importance of the mixed-phase cloud distribution in the control climate for assessing the response of clouds to carbon dioxide increase: a multi-model study. *Clim. Dyn.* 27(2-3), 113-126.
- Webb, M. J., C. A. Senior, D. M. H. Sexton, W. J. Ingram, K. D. Williams, M. A. Ringer, B. J. McAvaney, R. Colman, B. J. Soden, R. Gudgel, T. Knutson, S. Emori, T. Ogura, Y. Tsushima, N. Andronova, B. Li, I. Musat, S. Bony, K. E. Taylor, 2006: On the contribution of local feedback mechanisms to the range of climate sensitivity in two GCM ensembles. *Clim. Dyn.* 27(1), 17-38.
- Williams, K. D. and G. Tselioudis, 2007: GCM intercomparison of global cloud regimes: present-day evaluation and climate change response. *Clim. Dyn.* 29, 231-250.
- Wyant, M. C., C. S. Bretherton, J. T. Bacmeister, J. T. Kiehl, I. M. Held, M. Zhao, S. A. Klein, B. J. Soden, 2006: A comparison of low-latitude cloud properties and their response to climate change in three AGCMs sorted into regimes using mid-tropospheric vertical velocity. *Clim. Dyn.* 27, 261-279.
- Xie, S., M. Zhang, M. Branson, R. T. Cederwall, A. D. Del Genio, Z. A. Eitzen, S. J. Ghan, S. F. Iacobellis, K. L. Johnson, M. Khairoutdinov, S. A. Klein, S. K. Krueger,

W. Lin, U. Lohmann, M. A. Miller, D. A. Randall, R. C. J. Somerville, Y. C. Sud, G. K. Walker, A. Wolf, X. Wu, K.-M. Xu, J. J. Yio, G. Zhang, and J. Zhang, 2005: Simulations of midlatitude frontal clouds by single-column and cloud-resolving models during the Atmospheric Radiation Measurement March 2000 cloud intensive operational period. *J. Geophys. Res.* 110, D15S03, doi:10.1029/2004JD005119, 2005.

Yokohata, T., S. Emori, T. Nozawa, Y. Tsushima, T. Ogura and M. Kimoto, 2005: A simple scheme for climate feedback analysis. *Geophys. Res. Lett.* 32, L19703, doi: 10.1029/2005GL023673, 2005.

Figure legends

Figure 1

Mass ratio of liquid cloud water to cloud condensate in a model gridbox for the HS (dashed line) and LS versions (solid line), specified as a function of atmospheric temperature in the gridbox.

Figure 2

Zonal and annual mean of the cloud radiative forcing for ERBE (solid), HS(dotted), and LS(dashed); (a) shortwave and (b) longwave components. Units are in [W/m^2].

Figure 3

Zonal and annual mean of cloud ice content in height-latitude cross section; (a) HS, (b) LS, and (c) LS minus HS. Units are in [kg/kg]. Contours every 2×10^{-6} . Dashed lines indicate the isotherms of the control simulations from (a) HS, (b) LS, and (c) -5°C from HS and 0°C from LS.

Figure 4

(a) Shortwave cloud feedback for HS (solid curve), MS2 (dashed), and LS (dotted). Zonal and DJF mean. Units are in $[\text{W}/\text{m}^2/\text{K}]$. (b) Zonal and DJF mean cloud condensate response to CO_2 doubling for HS. (c) Same as (b) but for MS2. (d) Same as (b) but for LS. Units are in $[\text{kg}/\text{kg}]$. Contours every 3×10^{-6} . Negative values are indicated by dashed contours. Shading indicates the region where the CCTDs are calculated, which are displayed in Figure 5.

Figure 5

Response of cloud condensate (left panel) and CCTDs (right panel) to CO_2 doubling for the LS, MS2, and HS versions, averaged over the region indicated by the shading in Figure 4. (a) Condensation, evaporation, and precipitation. (b) Ice sedimentation. (c) Advection. (d) Cumulus mixing. (e) Dry convective adjustment. Units are in $[\text{kg}/\text{kg}]$ for the cloud condensate and in $[\text{kg}/\text{kg}/\text{s}]$ for CCTDs.

Figure 6

Temporal correlation between cloud condensate and the ice sedimentation term of the CCTD. The correlation is calculated using the DJF mean time series from the first 20 years after the instantaneous CO_2 doubling and is zonally averaged. The negative correlation is eliminated by assigning zero values in the figures. In addition, signs are switched to negative when the cloud responses are negative. The shaded area indicates the region where the CCTDs are calculated and displayed in Figure 5. Contours every 0.1. Negative values are indicated by dashed contours.

Figure 7

A conceptual model for the response of ice sedimentation to CO_2 doubling.

Figure 8

Vertical profile of cloud ice in the control run (thin curves) and its response to CO₂ doubling (thick curves), averaged over the latitudes 50°S–64°S, zonal and DJF mean. HS (solid), MS2 (dashed), and LS (dotted). Shaded area indicates the vertical range where CCTDs are calculated in Figure 5. Units are in [kg/kg].

Table

Table 1

Comparison of model physics between different model versions (HS, MS1, MS2, and LS). Model settings common to the LS version are shaded. Equilibrium climate sensitivities ΔT_{2x} are also listed for each version.

Model versions	HS	MS1	MS2	LS
(i) Mixed phase temperature range [°C]	-25, -5	-25, -5	-25, -5	-15, 0
(ii) Melted cloud ice	liq. cloud	liq. cloud	rain	rain
(iii) Parameter	fast*	slow*	slow*	slow*
ΔT_{2x} [°C]	6.2	6.4	5.3	4.1

* ‘fast’ and ‘slow’ correspond to different sets of parameter values; $(\alpha, V_0) = (0.04, 0.5)$

for the fast condition and $(\alpha, V_0) = (0.01, 0.25)$ for the slow condition.

Figure1

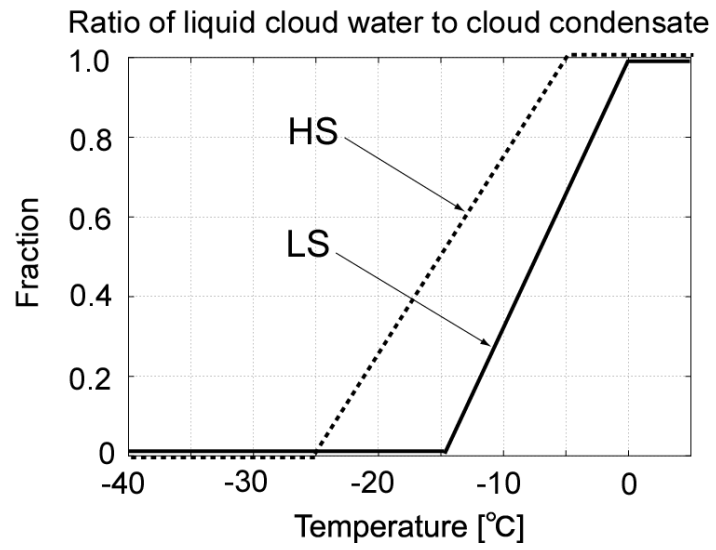


Figure 2

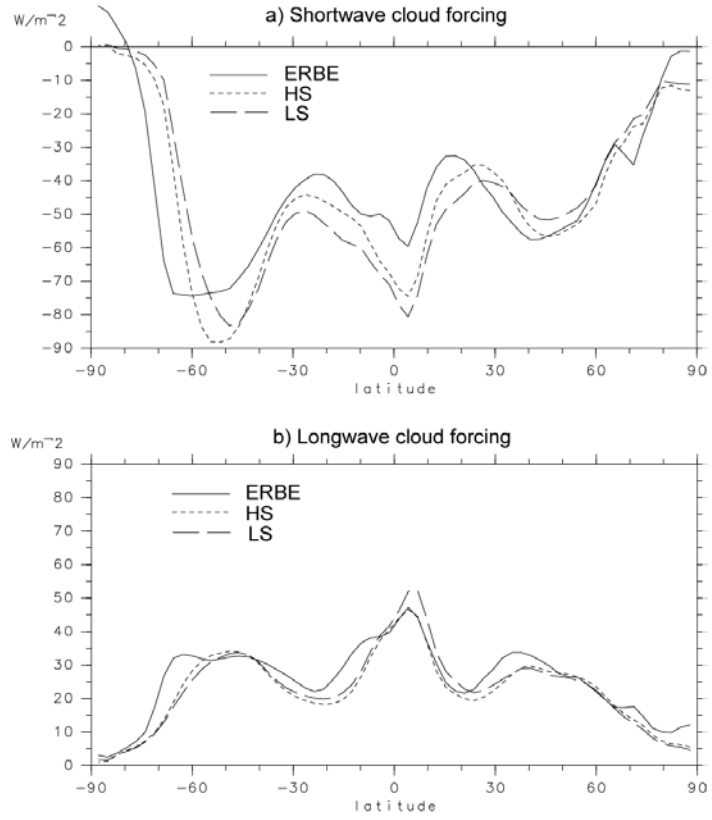


Figure 3

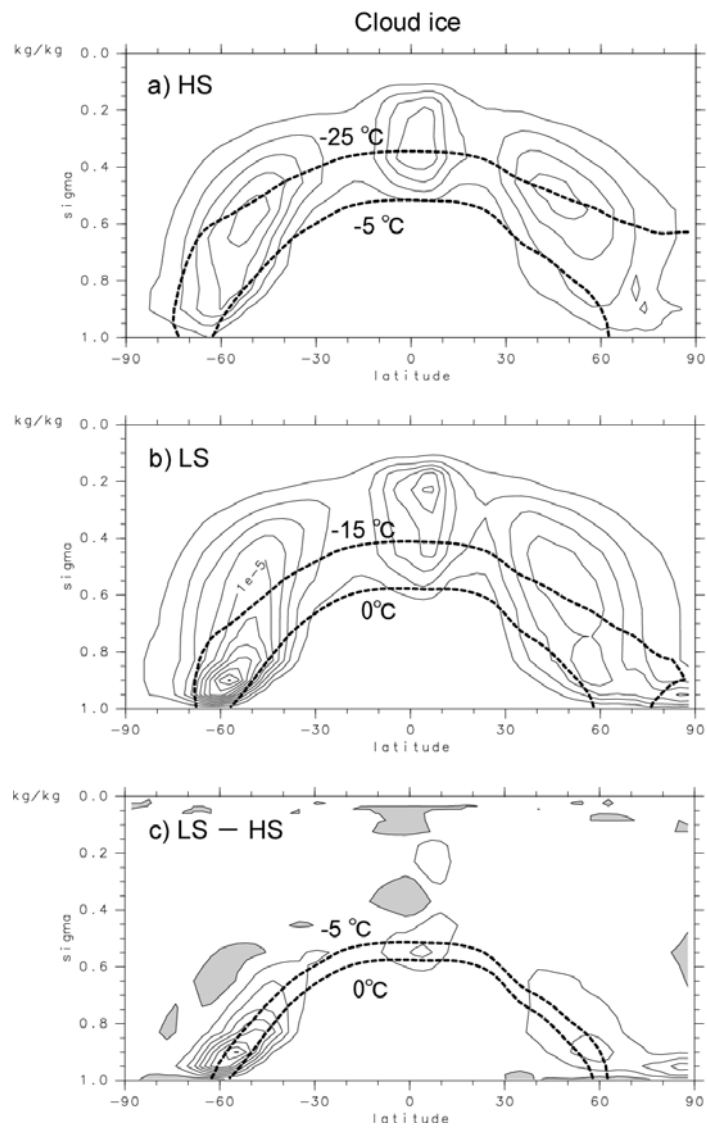


Figure 4

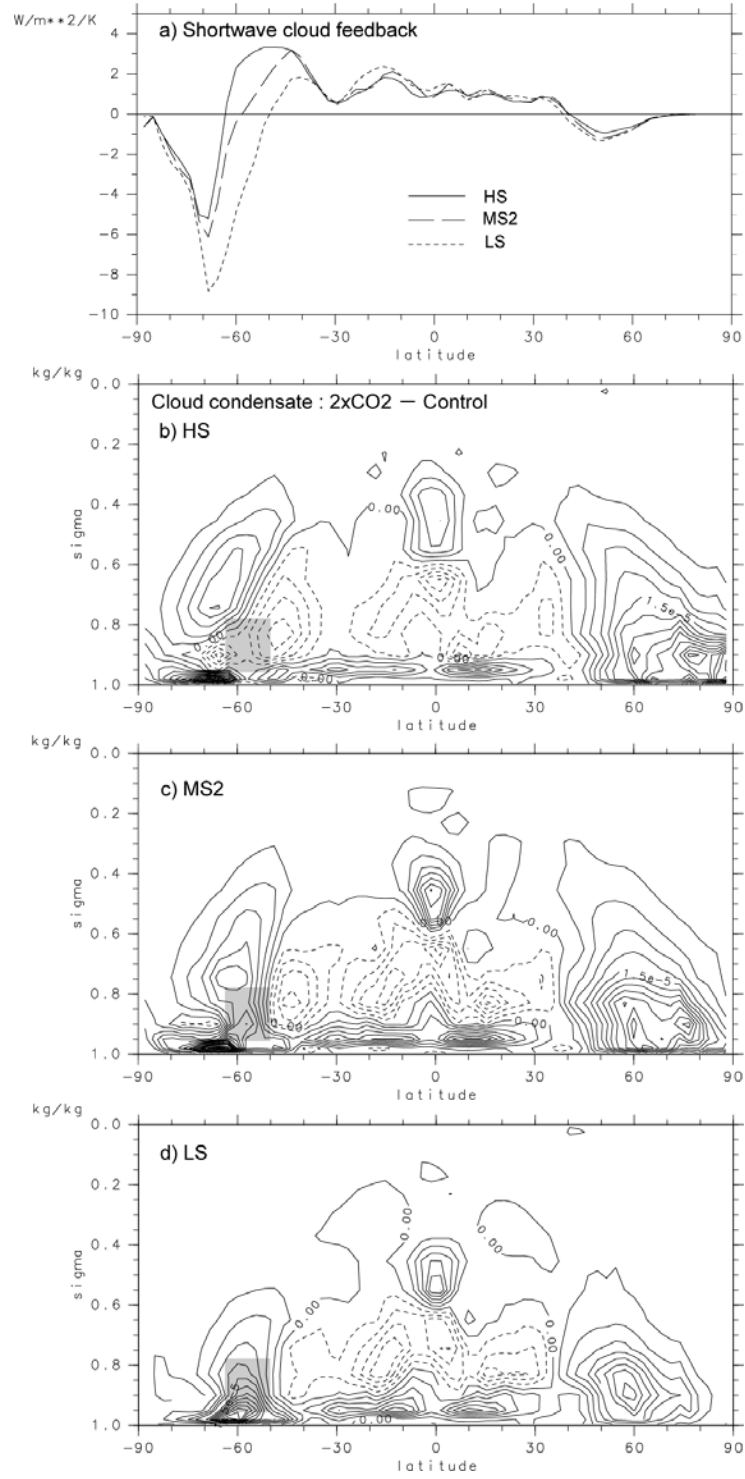


Figure 5

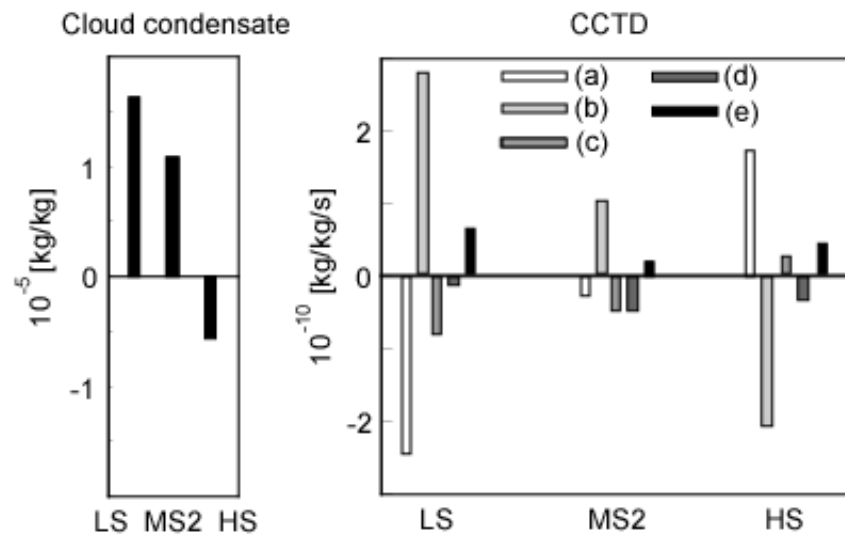


Figure 6

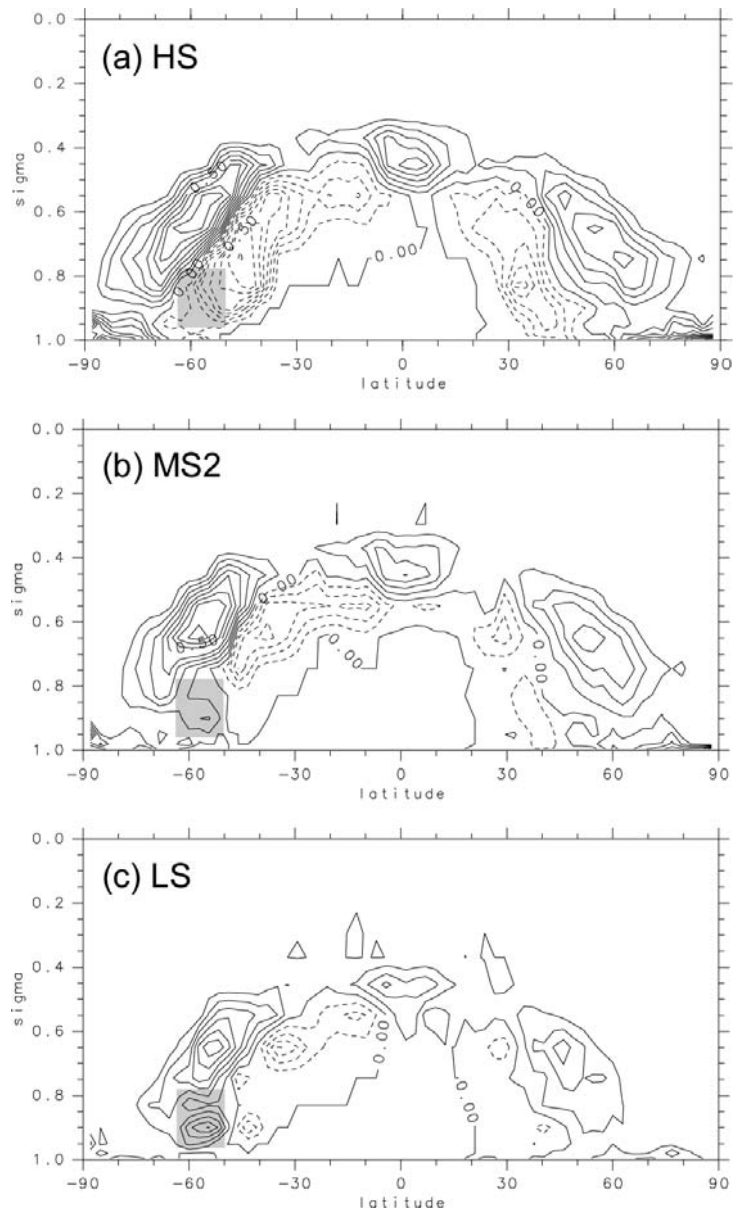


Figure 7

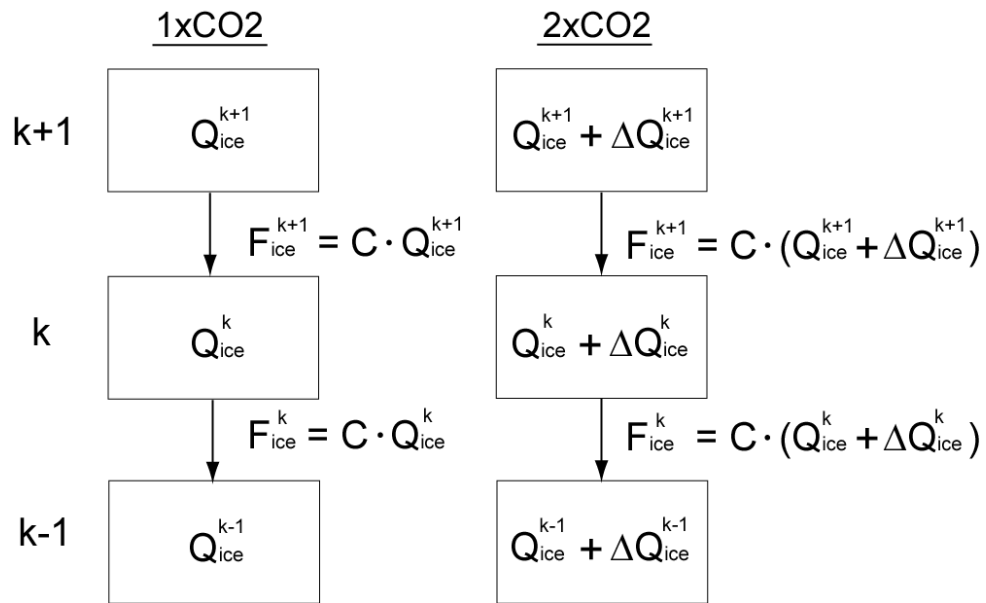


Figure 8

